UPS Battery Safety: Fire and Explosion Hazard Assessment and Mitigation

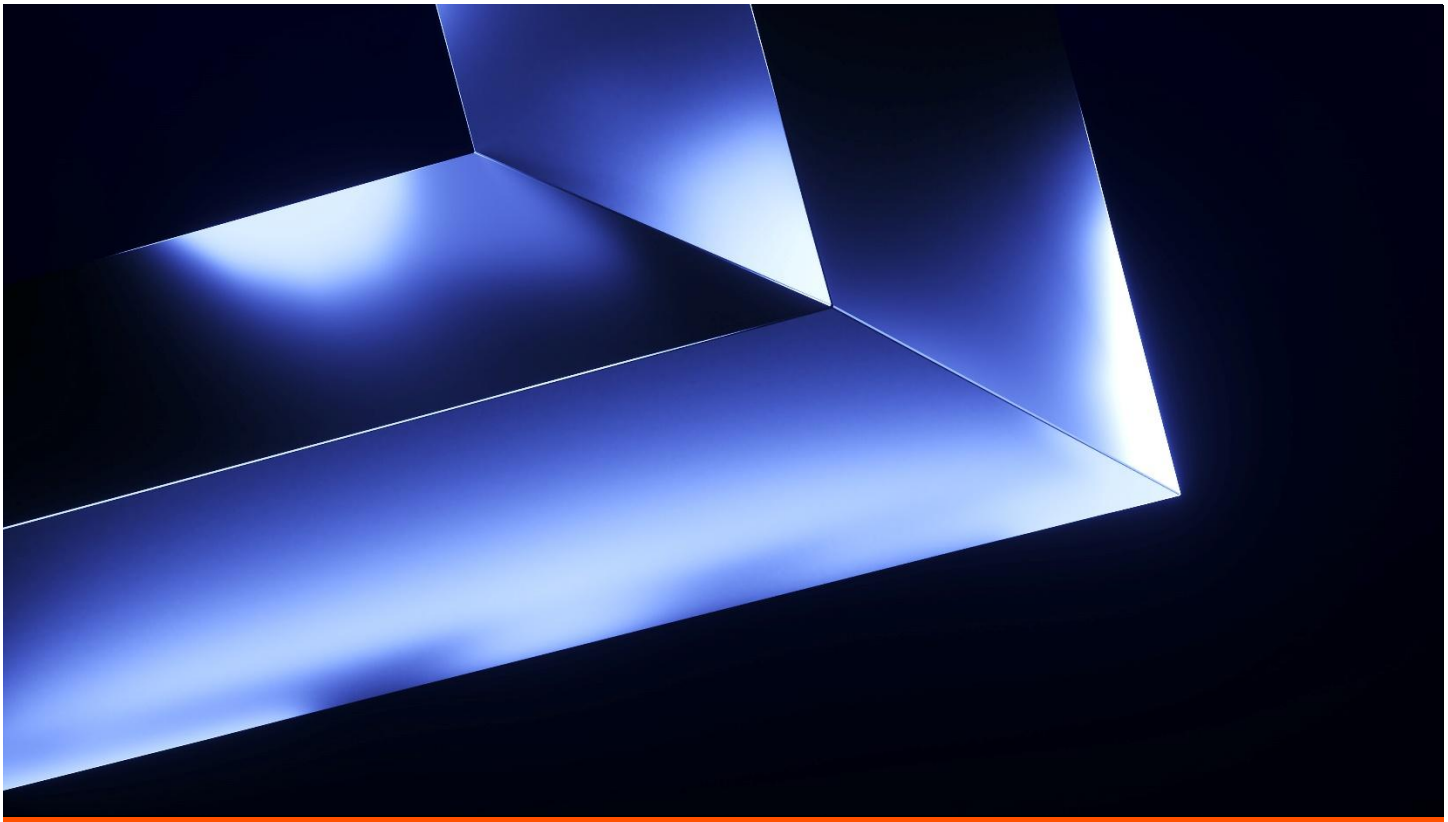

TECHNICAL REPORT

UPS Battery Safety: Fire and Explosion Hazard Assessment and Mitigation

Prepared by

Dong Zeng
Gang Xiong
Juan Cuevas
Regis Bauwens

FM
One Technology Way, Norwood, MA 02062

April 2026

Project ID: RW000938

Disclaimer

The research presented in this report, including any findings and conclusions, is for informational purposes only. Any references to specific products, manufacturers, or contractors do not constitute a recommendation, evaluation or endorsement by Factory Mutual Insurance Company (FM) of such products, manufacturers or contractors. FM does not address life, safety, or health issues. The recipient of this report must make the decision whether to take any action. FM undertakes no duty to any party by providing this report or performing the activities on which it is based. FM makes no warranty, express or implied, with respect to any product or process referenced in this report. FM assumes no liability by or through the use of any information in this report.

Executive Summary

Lithium-ion batteries (LIBs) are increasingly deployed in data centers as part of uninterruptible power supply (UPS) systems, presenting unique fire safety challenges. LIBs can act as both ignition and fuel sources, and fires involving them may lead to significant property damage and complicate firefighting efforts.

FM, in collaboration with Delta Electronics Inc. (hereafter referred to as Delta) and Equinix, conducted a comprehensive fire hazard evaluation of a LIB-based UPS battery system manufactured by Delta, ranging from cell-level characterization to installation-level large-scale fire testing. In Phase I, large-scale fire testing of the original system configuration showed that thermal runaway (TR) could propagate across two adjacent units. Based on these findings, the system design was modified, and the improved configuration successfully passed the Phase II large-scale fire test without TR propagation.

Phase I Testing – Original System:

The FM large-scale fire test was initiated by thermally abusing half of a module (10 cells, each with a nominal energy capacity of 60 Ah) to induce TR, with intentional ignition of the vent gases generated during TR. This approach triggered TR in the entire module, producing fire with a peak heat release rate (HRR) of approximately 700 kW.

The testing of three units revealed that TR in a single module could produce flames within the unit enclosure, leading to direct flame heating and TR propagation to adjacent modules. Although sprinklers were activated, the enclosure design restricted water access and reduced cooling effectiveness. Adjacent units experienced overheating, with module surface temperatures exceeding 500 °F (260 °C), the safety venting temperature, indicating the potential for TR propagation to the neighboring unit and the system failing the fire test, despite having shown compliance with UL 9540A.

Phase II Testing – Modified System:

In response to the results of Phase I, Delta collaborated with FM to redesign the UPS system with two key improvements:

- Reducing heat transfer to adjacent modules
- Enhancing sprinkler cooling effectiveness

Phase II fire testing used the same initiation scenario as that of Phase I. While a large flame was observed outside of the cabinet door, TR was confined to the initiating module. Neighboring modules remained undamaged, with surface temperatures below 212 °F (100 °C), significantly lower than the safety venting temperature. These results confirmed the effectiveness of the modifications, and the system passed the fire test.

Evaluation of Explosion Hazard

An explosion hazard analysis was conducted for the modified system under the scenario of a single module undergoing TR based on the fire testing results. In this scenario, the gas release would not present a significant room explosion hazard, limited to localized non-structural damage, and Damage Limiting Construction (DLC) would not be required when the system is installed in a room with an unoccupied volume greater than approximately 13,200 ft^3 (375 m^3), without supplemental mixing or ventilation. If the gas is well mixed and maintained below one-quarter of the lower flammability limit (LFL), the minimum volume can be reduced to 4,200 ft^3 (120 m^3), provided a minimum airflow of about 0.3 ft/s (0.1 m/s) is supplied across the exterior of the units. Alternatively, if continuous exhaust ventilation is provided at a minimum rate of 1 cfm/ft^2 (0.3 m^3/min/m^2), the required room volume can be adjusted to 8200 ft^3 (230 m^3), or as low as approximately 1,800 ft^3 (50 m^3) at 2 cfm/ft^2 (0.6 m^3/min/m^2) without the minimum mixing airflow requirement.

Conclusion:

The current FM large-scale fire test method captures realistic and conservative failure scenarios involving external ignition and module-level failure. Design enhancements developed through technical engagement among FM, Delta, and Equinix resulted in significant improvements to the fire safety performance relative to the initial configuration.

Abstract

Lithium-ion batteries (LIBs) used in uninterruptible power supply (UPS) systems present challenging fire and explosion hazards due to the potential for thermal runaway (TR) to produce both ignition sources and significant fuel. To address these risks in data center applications, FM developed a large-scale fire test method incorporating external ignition and module-level failure to evaluate the hazards of a Delta UPS system. The original UPS system in a typical battery room configuration exhibited full module involvement in TR with peak heat release rates near 700 kW, and heat transfer sufficient for TR propagation to adjacent racks, revealing limitations not identified by existing certification tests. Following targeted design modifications to reduce module-to-module heat transfer and enhance sprinkler cooling, the redesigned system was retested using the same method. TR remained confined to the initiating module, adjacent modules stayed below critical temperatures, and the system successfully met the new performance criteria. In addition, an explosion hazard analysis was performed to evaluate minimum room size and ventilation requirements. These results demonstrate that the current FM large-scale fire test method captures realistic and conservative failure scenarios involving external ignition and module-level failure. As part of a collaborative research effort involving FM, Delta, and Equinix, a modified LIB UPS system was evaluated using the FM large-scale fire test. The system successfully passed the test under the specified conditions.

Acknowledgements

The authors would like to acknowledge John Hamblin and Denise Schlitt of Equinix; Tib Lin, Clyde Chiu, York Tsai, Charles Chang, and Geoffrey Dai from Delta Electronics Inc., Dr. Yi Wang, Dr. Marcos Chaos, Ben Ditch, Adrian Oxley, Bob Kasiski, Errol Lau, Nicholas Cummings, and Helen Sheng from FM, and James Dobson and Jagdev Mavi from the Bureau of Fire Prevention for the City of San Jose. The test teams from the FM Research Campus' Small Burn Lab and Large Burn Lab conducted the experiments. Their efforts are sincerely appreciated.

Table of Contents

List of Figures

List of Tables

1. Introduction

Lithium-ion batteries (LIBs) are increasingly used in data centers as part of uninterruptible power supply (UPS) systems. They are typically housed in cut-off rooms protected by the building's sprinkler system. Failure of LIBs can result in the release of flammable gases and significant heat, posing both fire and explosion hazards. A fire or explosion involving LIBs within a building can lead to significant property damage and present serious challenges for firefighting operations.

Currently, the fire hazards of LIB UPS systems are evaluated using the UL 9540A testing methodology [1], which assesses thermal runaway (TR) and fire spread across cell, module, and unit levels in battery energy storage systems. While results obtained in UL 9540A testing provide valuable insights into system performance during TR, additional testing approaches are necessary for scenarios in which UPS installations may be exposed to ignition sources commonly found in data center environments. In some UPS room configurations, flammable vent gases released during TR may encounter external ignition sources, such as electrical equipment or localized fires involving other combustibles. Such conditions may alter gas combustion behavior, heat release, and overall fire dynamics. Moreover, the minimum initiation conditions assumed in many standardized protocols may differ substantially from practical scenarios, in which TR in an operational system may involve a larger fraction of a module or multiple cells simultaneously.

As data centers continue adopting LIB UPS systems, Authorities Having Jurisdiction (AHJs), operators, and manufacturers have shown increasing interest in large-scale testing methods that more directly represent these conditions, including scenarios involving external intentional ignition, to better capture the fire hazards of LIB UPS installations.

To address this need, FM collaborated with Delta to conduct a comprehensive fire hazard assessment and evaluate design improvements of a LIB UPS battery system intended for use by Equinix, a global data center operator. The assessment employed installation-level large-scale fire testing with intentional ignition of vent gases to represent credible worst-case scenarios, along with cell-level and module-level characterizations. This report summarizes the test results and hazard analyses for consideration by AHJs.

This report is organized as follows. Section 2 provides an overview of the original LIB UPS system and UL 9540A test results [2, 3]. Section 3 introduces the large-scale fire test methodology developed in the present work, followed by a detailed comparison of the original and modified systems, including the rationale and impact of the design changes. Section 4 presents a theoretical analysis of the potential explosion hazards posed by the system, and Section 5 summarizes the key findings and conclusions.

2. The Original LIB UPS System and UL 9540A Testing Results

2.1 The Original UPS System

The original LIB UPS battery unit examined in this work, shown in Figure 2-1(A), is manufactured by Delta, model BSPRU-DE1072P0GL0. Each unit comprises two safety control boxes and 14 modules, designated as BSPMU-DE1201C0GL0, arranged in two separate seven-module strings, each featuring a 140S1P cell configuration. Each unit possesses a nominal energy capacity of 62.1 kWh, a nominal voltage of 518 Vdc, dimensions of 26.3 × 94.8 × 34.4 inches (668 × 2407 × 873 mm) (W × H × D), and a weight of 2094 lb. (950 kg). The side walls and front door consist of solid steel plates, whereas the back wall is constructed from a perforated steel plate. The top cover of the unit features an opening that reveals two pairs of bus bars.

Each module has a nominal energy capacity of 4.44 kWh, a nominal voltage of 74 V, measures 28.4 × 7.7 × 8.5 inches (722.4 × 195 × 216.4 mm), and weighs 84 lb. (38 kg). Each module comprises 20 LIB cells, model number P140-222-0 (P140). Figure 2-1(B) shows the configuration of the module. The cells are situated within plastic scaffolding composed of polycarbonate and acrylonitrile butadiene styrene (PC-ABS). The plastic scaffolding serves to isolate the cells from one another and from the module case, which may lead to a decrease in heat transfer rates. The top cap of the plastic scaffolding features a chimney that facilitates the venting of TR effluent gas to the exterior of the module. The remainder of the module consists primarily of metal, with certain combustible materials in the electrical insulator layer, as illustrated in Figure 2-1(B), along with plug-in connectors and external handles.

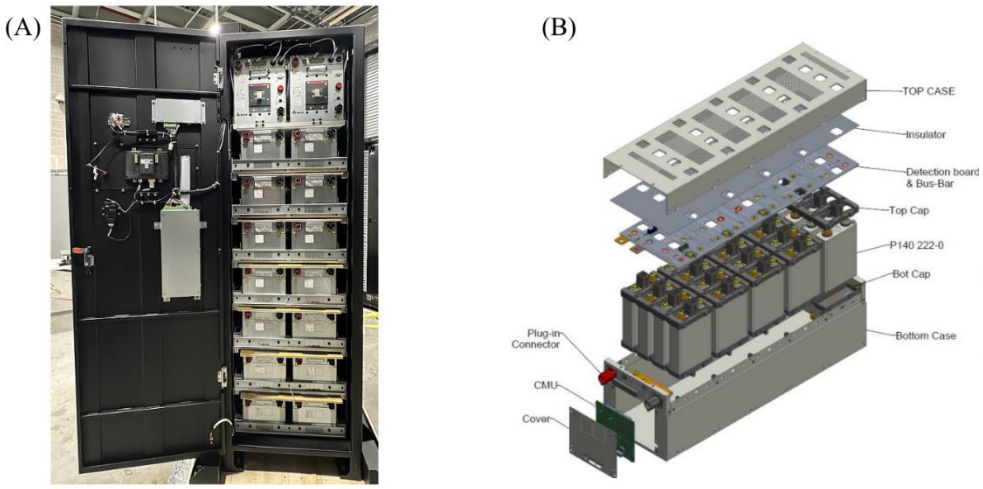

Figure 2-1: Delta UPS battery system, (A) Image of Delta's BSPRU-DE1072P0GL0 LIB unit, (B) Layout of Delta's BSPMU-DE1201C0GL0 module.

The P140 is a prismatic cell featuring a lithium nickel manganese cobalt oxide (NMC) cathode and a graphite anode, with electrical ratings of 3.7 V and 60 Ah. The dimensions are 6.1 × 4.3 × 1.5 inches (155.6 × 110.1 × 38.2 mm), and the weight is approximately 3.1 pounds (1.4 kg). The cell features a vent port located at the center of its upper surface. The vent port aligns with the chimney of the top cap of the plastic scaffolding when installed in the module.

2.2 Summary of UL 9540A Testing

The fire hazards associated with the P140 cell, the BSPMU-DE1201C0GL0 module, and the BSPRU-DE1072P0GL0 unit were assessed by an external laboratory utilizing the UL 9540A test method (2019 version) [4]. Although the UL 9540A test has known limitations, its results offer valuable insights into TR propagation between cells, particularly in scenarios where one cell attains TR without producing a flaming condition. The TR propagation characteristics observed at both the module and unit levels were found to be comparable, with TR confined to the initiating module; therefore, the detailed unit-level test setup for the remaining units is not discussed here, and only the unit-level test results [3] are considered.

In the UL 9540A unit-level test, all modules were charged to a 100% state-of-charge (SOC) and one module was designated as the initiating module. A single cell within this module was thermally abused to initiate TR. Within the initiating module, a cell located at the center of the module (highlighted by the red circle in the post-test image in Figure 2-2), was heated at a rate of 5.5 °C/min via electrical heaters. TR occurred after approximately 21 minutes, releasing a substantial amount of gas that enveloped the unit. TR did not propagate to adjacent cells, likely due to reduced heat transfer caused by the separation between cells. The post-test image of the initiating module (Figure 2-2) indicated that the damage was largely confined to the cell of origin, while neighboring cells exhibited minimal damage.

Figure 2-2: Post-test image of the initiating module [3].

However, inducing TR in a single cell without intentionally igniting the vent gas does not constitute a worst-case failure scenario under real-world conditions. Therefore, FM conducted a comprehensive fire hazard assessment of the UPS system, as discussed in the following section.

3. FM Large-scale Fire Testing

To evaluate a realistic failure scenario under representative conditions, FM developed a targeted initiation method and a large-scale fire test protocol. Phase I testing was conducted using the original UPS system design. The test results revealed significant fire hazards, including potential TR propagation to adjacent units. Based on insights learned from Phase I, the system was redesigned to mitigate these hazards. The modified version was then subjected to Phase II testing, which it successfully passed. This section outlines the test methodology, compares results from both phases, and discusses the underlying physical mechanisms driving TR propagation and fire development.

3.1 Initiation Method

In a LIB UPS battery room, combustible materials include LIB cells and modules, electrical cables, and various components associated with the UPS equipment. Fires may originate from failures in electrical systems, TR of cells or modules, or external ignition sources involving nearby combustibles. In the absence of system-level malfunctions, the likelihood of simultaneous failure of multiple modules is considered low. Therefore, TR initiation from a single battery module is deemed to be a realistic and representative scenario for system-level fire testing.

In this study, TR was initiated in half of a module, i.e., 10 cells within a 20-cell module. To validate this initiation method, a module-level test was performed using two fully charged modules (100% SOC) placed side by side. A mock-up fixture was used to secure the modules and mimic enclosure conditions typical of actual unit installation. The second module was positioned adjacent to the initiating module, maintaining the same separation distance as in the real unit. A glow plug was placed between the front face of the initiating module and the mock-up door to ignite flammable gases produced during TR, aligning with the gap between the module's top cover and the rack tray. Additionally, a supplementary glow plug and premixed pilot flame were used. The test assembly was placed under a calorimeter to measure chemical heat release rate (HRR), as shown in Figure 3-1 (A). Further setup details are available in Appendix A.

Ignition of the vent gases produced during the induced TR in the initiating module produced a flame approximately 8 ft. (2.4 m) in length, as illustrated in Figure 3-1(B). Unheated cells in the initiating module subsequently underwent TR, leading to small-sized fires, as shown in Figure 3-1(C). Post-test inspection confirmed that all 20 cells in the initiating module experienced TR, but no propagation occurred to the adjacent target module.

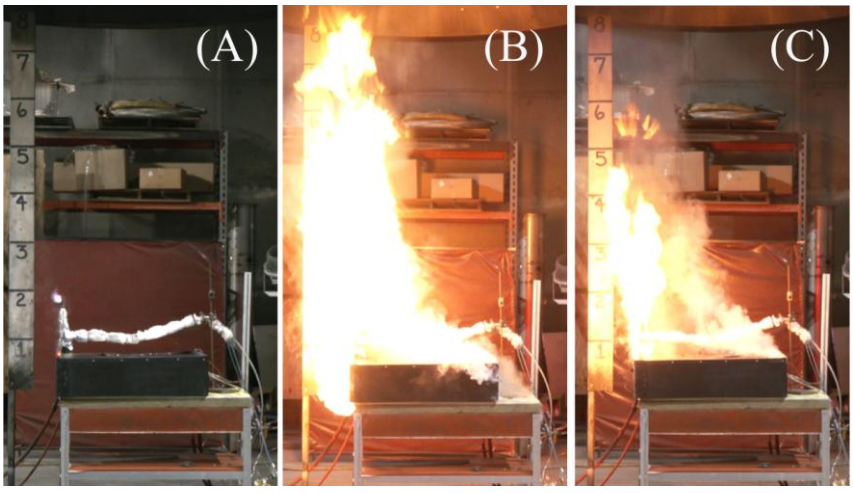

Figure 3-1: Side-view of test images, (A) before ignition, (B) at approximately the maximum fire size, (C) flame image corresponding to a subsequent TR event at ~23 minutes. Note two modules are placed side by side.

The HRR data presented in Figure 3-2 illustrates the TR process described above. The maximum HRR occurs approximately 15 minutes into the test, coinciding with the initial TR of the thermally abused cells. Subsequently, smaller HRR spikes are associated with TR events in cells located farther from the heaters. The integration of the HRR curve yields a total heat release of 135 MJ, providing a quantitative measure of the energy released during the full TR event of the initiating module.

In summary, the module-level test validated the efficacy of the chosen initiation method, which successfully induced TR in all cells within the initiating module. The event produced a peak HRR of approximately 700 kW, accompanied by sustained fire behavior. Given the results, the initiation method was deemed suitable for use in installation-level tests to simulate realistic failure scenarios.

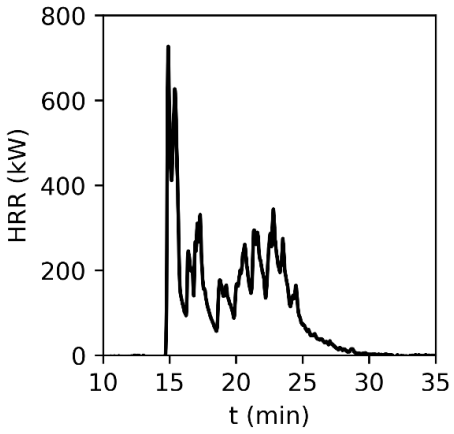

Figure 3-2: Chemical HRR of the module-level fire test.

3.2 Large-scale Fire Test Design

3.2.1 Overview of the Test Setup

A large-scale, installation-level fire test method was developed to assess the fire hazards associated with LIB battery units located within a sprinklered UPS room. The test protocol was designed to assess three critical aspects: TR propagation, fire propagation, and the effectiveness of sprinkler systems in suppressing fires in LIB systems. In the present study, the test configuration comprised one UPS unit of origin and two adjacent target UPS units, all situated beneath representative ceiling-level sprinklers within a mockup room to reflect typical installation conditions.

Three UPS units were installed within a mockup room measuring 20×10×10 ft (6.1×3.05×3.05 m), as shown in Figure 3-3. The room featured partial walls extending 3 ft (0.9 m) down from the ceiling on the front and right sides (Figure 3-3(D)), constructed from 5/8-inch (16 mm) gypsum wallboard. The two side walls were left partially open to mitigate deflagration hazards and to enable observation of compartment fire effects, including the formation of a hot ceiling layer. As a result, the potential effects of underventilation in a closed enclosure were not directly evaluated in this test. The entire setup was placed beneath FM's Large Burn Lab 20 MW calorimeter to enable measurement of HRR.

Ceiling-level sprinklers were installed with a spacing of 10 ft (3.05 m), maintaining a distance of 5 ft (1.5 m) from the side and rear walls, as illustrated in Figure 3-3(C). The sprinklers were a standard response type with a nominal K-factor of 8 gpm/psi$^{1/2}$ (115 L/min/bar$^{1/2}$) and a design water density of 0.3 gpm/ft^2 (12 mm/min). The thermal link of the sprinklers was positioned 12 inches (0.3 m) below the ceiling. In Phase I, the sprinkler activation temperature was 212 °F (100 °C). In Phase II, the activation temperature was 165 °F (74 °C), but with simulated thermal links to track the temperature history of the sprinklers.

The UPS unit of origin was positioned one inch (25 mm) from the back wall of the room ("c" in Figure 3-3(B)). Two target units were positioned on both sides of the unit of origin, with a separation of 1 inch (25 mm) from it ("b" in Figure 3-3(A)). This configuration is considered representative of actual installations.

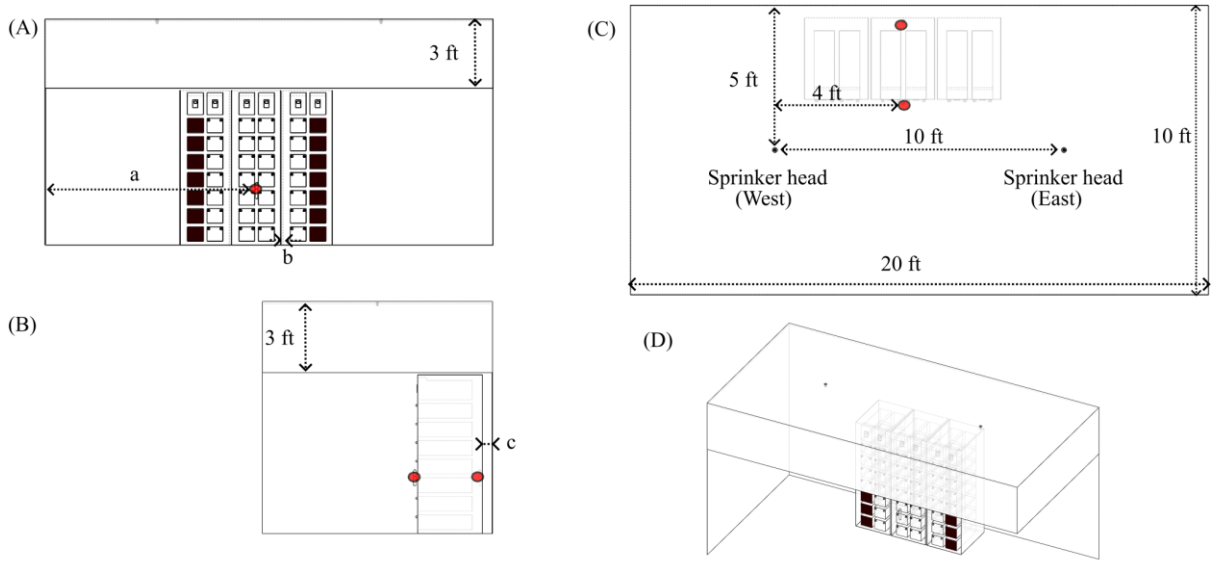

Figure 3-3: Illustration of test configuration of a large-scale fire test for LIB racks installed inside a UPS room, (A) front view, (B) side view, (C) plan view, (D) isometric view. Red dots indicate the locations of glow plugs, black squares represent empty module space.

The third module from the bottom within the unit of origin (shown in Figure 3-4) was selected as the initiating module. This location facilitates the examination of both upward and downward vertical flame spread. The lateral distance from this module to the nearest sprinkler was 4 ft. (1.2 m). TR initiation followed the procedure outlined in Section 3.1, with glow plugs installed above the initiating module to ignite the flammable gases released during TR, as illustrated in Figure 3-3.

From a fire hazard perspective, the propagation of fire and TR should be confined to the unit of origin. To evaluate this, the following failure criteria are defined:

(1) The temperature of adjacent units, as measured by thermocouples positioned on the selected module surfaces, reaches or exceeds the cell venting temperature of 500 °F (260 °C), as determined in cell-level tests (see Appendix B).

(2) The occurrence of TR or reignition in any batteries within a 24-hour observation period following the termination of the test.

3.2.2 Module Setup in Phase I and Phase II Tests

To facilitate subsequent discussion, module identification numbers are provided in Figure 3-4. The modules within the unit of origin are numbered 15 to 28, with Module 23 designated as the initiating module.

In the Phase I test, the unit of origin was fully populated with modules, while the target units were partially filled (50%), containing only the modules closest to the unit of origin; all cells were charged to 100% SOC. To minimize personnel exposure to electrical hazards, only the top three modules of each string in all units were electrically connected. All unit doors were closed prior to the start of the test to replicate normal operational conditions.

In the Phase II test, the same initiation method was used, but with a reduced number of modules based on lessons learned from the Phase I test. In addition to the initiating module (23), six modules (17, 19 – 22, and 24) were fully populated and charged to 100% SOC. Nine modules (2, 15, 16, 18, and 25 – 29) were installed empty (with all cells removed). The effect of such a configuration is discussed in Section 3.3.4.

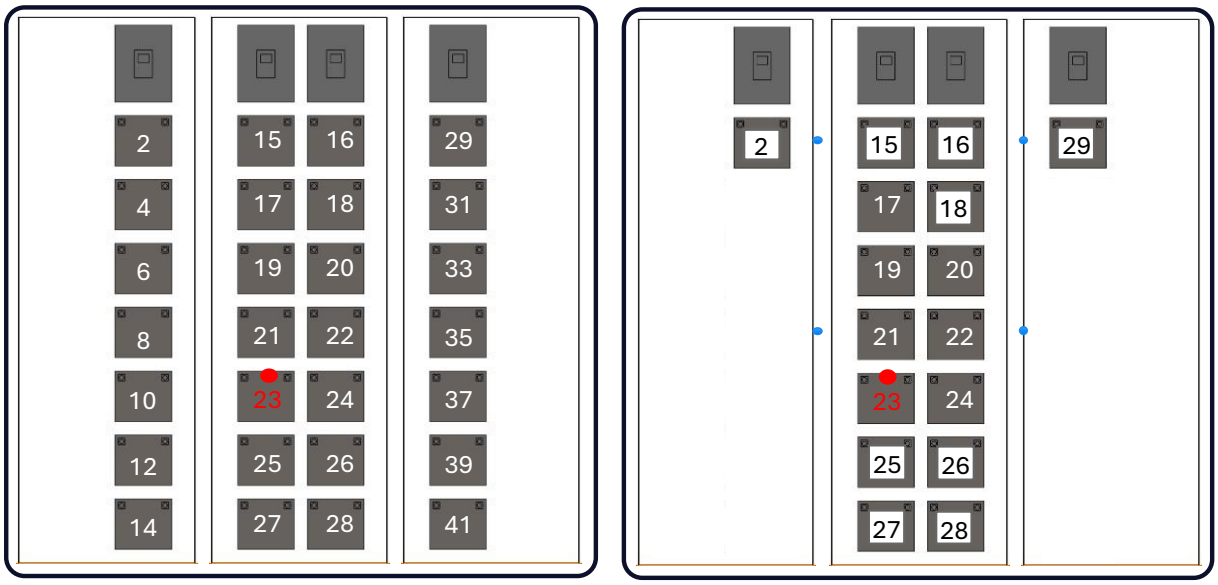

Figure 3-4: Module setup for Phase I (left) and Phase II (right) tests. Module 23, highlighted in red, is the initiating module; the red circle shows the location of the glow plug; modules marked with white filling are empty.

3.3 Phases I and II Test Results

3.3.1 Fire Growth History and TR Propagation

Figure 3-5 shows the fire growth histories for both Phase I and Phase II tests. In the Phase I test, the HRR rapidly increased, reaching a peak of about 800 kW at around 17 minutes. This was followed by a decline to a low value at 22 minutes and remained low until the 30-minute mark. The Phase II test exhibited a similar fire growth pattern during the first 30 minutes. In both cases, the HRR trend closely resembles the HRR profile observed in the module-level test (shown as red dotted line with time-shifting to match the onset), confirming the dominant role of Module 23 in early fire development.

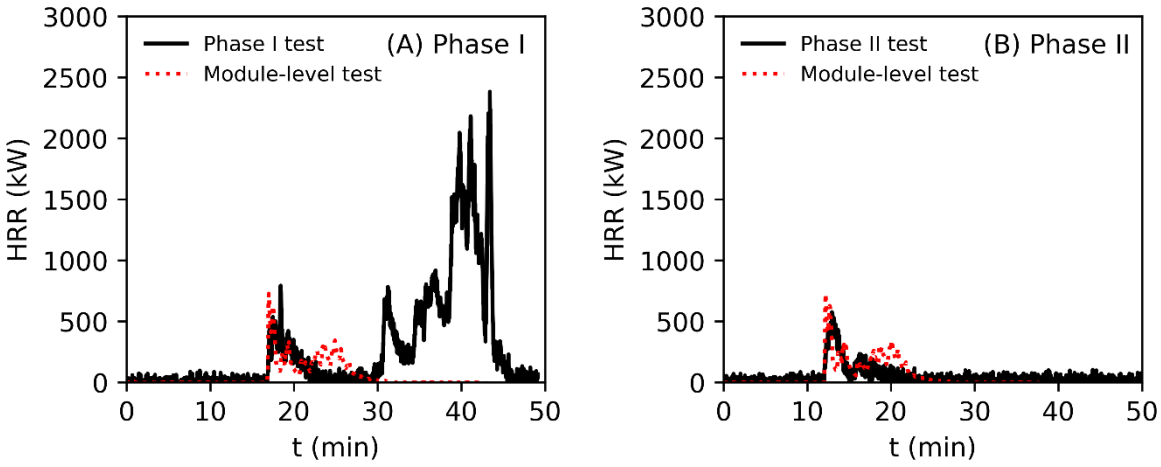

Figure 3-5: Heat release rate (HRR) of the three-unit fire tests, with module-level result shown as red dotted lines.

Despite displaying similar initial fire growth, the two tests diverged significantly after 30 minutes. In the Phase I test, the HRR rose again at around 30 minutes, reaching another local peak of about 800 kW. This was followed by a number of local peaks, suggesting the involvement of additional modules and TR propagation within the unit of origin. At around 38 minutes, the surface temperatures of Modules 2 and 29 in the target units exceeded the cell venting temperature of 500 °F (260 °C), as

shown for Phase I in Figure 3-6; thereby meeting the test failure criteria. Although the automatic sprinklers activated at approximately 24 minutes, they were ineffective in suppressing the TR propagation process. This is likely caused by the unit enclosure obstructing water access to the modules. The HRR ultimately reached a maximum value of 2400 kW before manual suppression was initiated and the test was concluded. Post-test monitoring over a 24-hour period confirmed that no further reignition or TR events occurred.

In contrast to Phase I, the Phase II test showed no visible flames after 24 minutes, and the HRR remained consistently low throughout the remainder of the test. Thermocouples mounted on the target unit walls (see Appendix C for detailed sensor locations) recorded maximum temperatures below 212 °F (100 °C) (see Figure 3-6), indicating no TR propagation potential to neighboring units in the Phase II test.

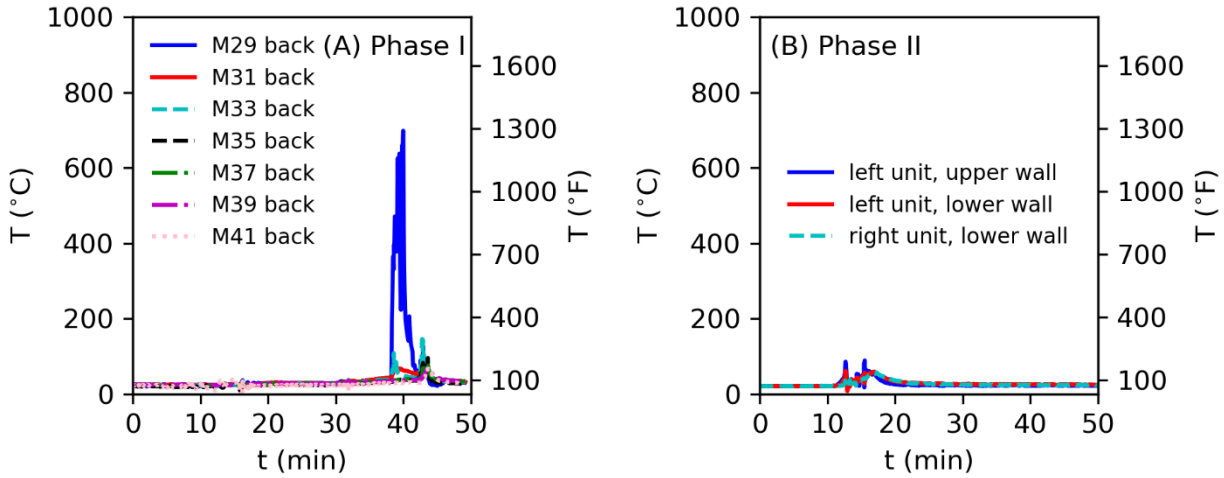

Figure 3-6: Temperature history in the target units for Phase I and Phase II tests.

Post-test inspection showed that the unit of origin sustained significant thermal damage in the Phase I test (see Figure 3-7). The front surfaces of Modules 23 and 24, along with those positioned above them, showed visible thermal damage. Internal components, such as plastic caps, demonstrated signs of charring and heat-induced damage. Close examination of Modules 15 to 24 showed that most of their cells had undergone venting, as evidenced by open vent ports. However, the bottom four modules maintained a measured voltage of 80 V, confirming that TR did not propagate to them.

Figure 3-7: Images of the unit of origin and measured voltages after tests, left: Phase I test, right: Phase II test.

In contrast, the Phase II test resulted in damage confined solely to the initiating Module 23, with a measured voltage of 0 V post-test. All other full modules maintained a voltage of 80 V, demonstrating no TR propagation. In addition, plastic caps and cables located in front of all modules (except Module 23) showed only minor discoloration, suggesting minimal thermal exposure.

In summary, Phase I and Phase II tests used the same evaluation methodology and showed similar initial fire growth from the initiating module. However, the original UPS system tested in Phase I exhibited TR propagation and failed the test, while the modified UPS system tested in Phase II successfully contained the fire within the initiating module and passed the test. The following sections discuss the lessons learned from the Phase I test and how these insights informed the redesign of a safer UPS system with improved fire performance.

3.3.2 Lessons Learned from Phase I Testing and Redesign of the UPS System

Although the original UPS system did not exhibit fire spread hazards under UL 9540A test conditions, it failed the FM large-scale fire test. One key differentiator is the initiation method. Unlike the UL 9540A scenario which involves no intentional ignition, the FM test initiated TR in 10 cells within a module and intentionally ignited the vent gases using glow plugs. This initiation resulted in a fire with a peak HRR of approximately 700 kW during the TR event in the initiating module.

The intentional ignition of vent gases significantly increases fire severity. As evidenced by the cell-level testing shown in Appendix B, the combustion of vent gases generates heat release rates that are approximately six times those measured in unignited scenarios. This highlights the elevated fire hazard posed under more realistic conditions. The outcomes of the large-scale fire tests developed at FM suggest that this testing protocol is more effective in evaluating the fire hazards associated with UPS battery units. It simulates a reasonably conservative scenario and could serve as the basis for a standardized fire testing procedure for LIB UPS battery systems.

To further understand the hazard mechanisms, a detailed heat transfer analysis was conducted. During TR of Module 23, vent gases burned within the cavity formed between the front door and module surfaces. This was confirmed by a camera positioned inside the cavity, observing from below (see Figure 3-8). As TR progressed and more cells became involved, the amount of vent gases increased. The confined space and limited oxygen availability led to partial combustion within the cavity and release of unburned gases outside the initiating unit, resulting in a ceiling-level fire that activated sprinklers. The TR propagation in Module 23 lasted approximately 10 minutes, as indicated by the module-level test results. Although external flaming subsided, the cavity flame likely persisted, providing sustained heating that ultimately triggered TR in adjacent modules, leading to additional effluent gas and a larger fire.

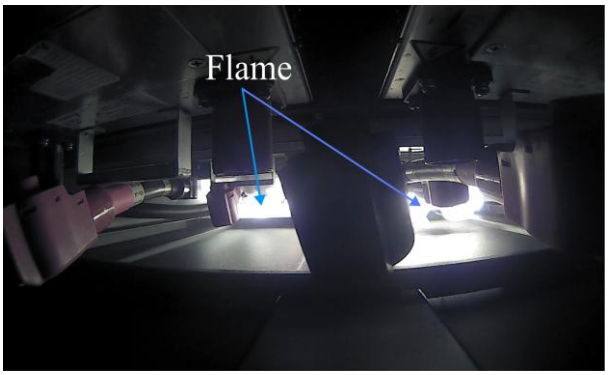

Figure 3-8: Cavity flames appear between the front door and the module front surfaces of the initiating unit, captured by a camera placed inside the cavity viewing from the bottom of the cavity. The subject in the middle of the view is an electrical cable connector.

Figure 3-9(A) shows a cross-sectional schematic illustrating the dominant heat transfer mechanisms within the unit of origin, using a representative string comprising Modules 15, 17, 19, 21, 23, 25, and 27. Visible flames were observed at the ceiling level, along with cavity flames inside the unit enclosure during the TR event. The schematic highlights two main heat transfer pathways:

(1) Module-to-module heat transfer ($\dot{Q}_{sen}$): Heat generated internally by cells undergoing TR raises the temperature of the reacting module and transfers heat to adjacent modules.

(2) Flame heat transfer ($\dot{Q}_f$): Flammable gases released during TR ignite within the unit cavities, distributing heat simultaneously to multiple modules.

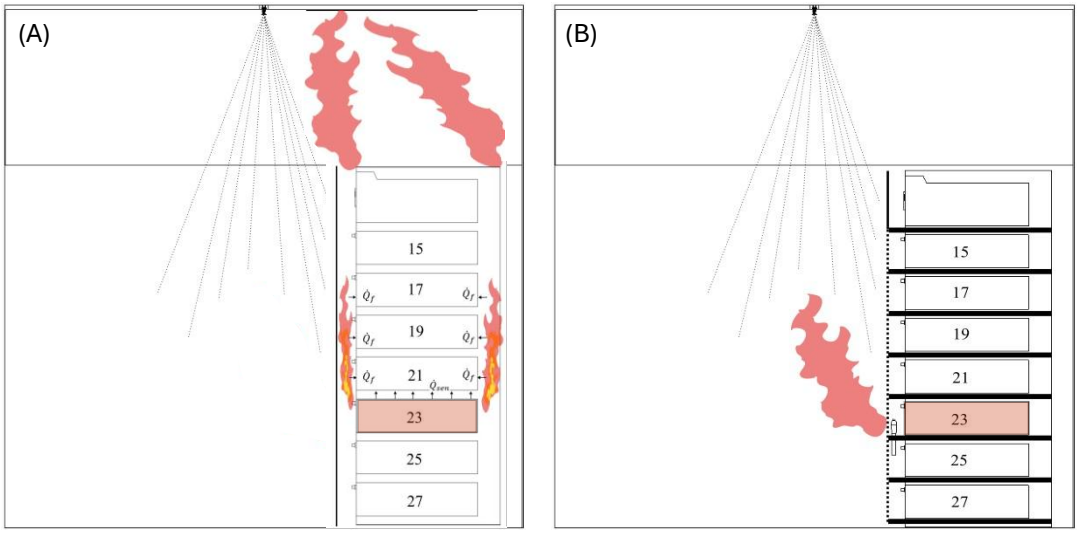

Figure 3-9: Cross-section illustration of the heat transfer mechanisms in (A) original UPS system in the Phase I test and (B) modified UPS system in Phase II test (see text for a list of modifications).

TR propagation within the initiation unit is believed to have been accelerated by the cavity fires, which heated multiple modules simultaneously. Compared with module-to-module heat transfer, which affects only adjacent modules, the cavity fire exerted a far greater influence on event escalation. This conclusion is supported by the observations provided in Section 3.3.3, where multiple modules above Module 23 exhibited significant temperature increases. This analysis suggests that the cavity fire, driven by the combustion of flammable gases released during TR, was the dominant mechanism contributing to the rapid escalation of the event.

Based on these findings, several enclosure-level design modifications were implemented to mitigate fire propagation hazards, as shown in Figure 3-9(B):

1. Each module was physically compartmented, and the unit door was perforated to redirect TR vent gases away from adjacent modules and limit air entrainment, thereby reducing the likelihood of cavity fires.
2. The unit's side walls were removed to enhance the heat dissipation and improve sprinkler application by facilitating water access to heated surfaces.
3. Insulation walls were added between adjacent modules to reduce the inter-module heat transfer, limiting the potential for TR propagation.

It is important to note that these modifications were applied solely to the enclosure configuration. The battery modules themselves remained unchanged in the modified UPS system.

3.3.3 Detailed Comparison between Phase I and Phase II Tests

Figure 3-10 shows images captured during the Phase I and Phase II tests. In the Phase I test image, the flame is largely obscured by the unit doors and adjacent units, while in the Phase II image, a prominent flame is clearly visible in front of the perforated unit door. At the time of imaging, the HRR measurements were approximately 300 kW for the Phase I test and 200 kW for the Phase II test. The limited flame visibility in Phase I is attributed to the cavity fires occurring within the enclosure, which were concealed by the closed doors. Conversely, in Phase II, despite the lower HRR, the flame was external and unobstructed, resulting in a greater visual prominence.

Figure 3-10: Images of the test at ~17 minutes in Phase I and ~12 minutes in Phase II tests.

The difference in the flame location is also reflected in the thermocouple measurements. Figure 3-11(A) shows temperature measurements from the initiating unit, with thermocouples on the front surfaces of Modules 15 to 28 (with detailed locations shown in Appendix C). Around 17 minutes into the Phase I test, coinciding with TR of module 23, temperatures for all modules rose sharply, reaching up to 1472 °F (800 °C). This indicates active flaming from the combustion of TR gases. As shown in Figure 3-8, cavity fires formed as these gases burned within the enclosure. Rear-surface temperatures exhibited similar trends, suggesting that cavity fires were present behind the modules as well. Such cavity fires posed direct flame heating to modules above Module 23, contributing to continued TR propagation and elevated HRR.

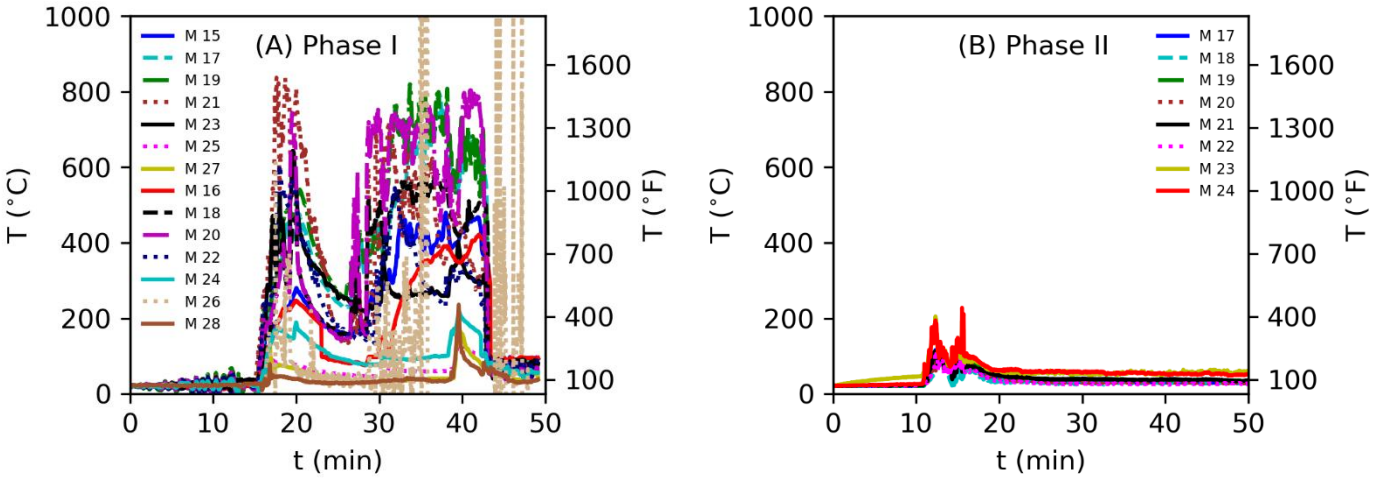

Figure 3-11: Temperatures inside the enclosure, (A) front surface temperatures of the modules in the initiating unit in the Phase I test, (B) front door (inner side) temperatures above different modules in the Phase II test.

Notably, the surface temperatures of Modules 25 – 28, located beneath Module 23, remained below 236 °C, supporting the conclusion that buoyancy-driven cavity fires were the dominant heat transfer mechanism, while radiative and conductive module-to-module heat transfer played a less significant role.

In the Phase II test, thermocouples mounted on the inner side of the front door (see Figure 3-11(B)) recorded temperatures below 446 °F (230 °C) throughout the test (see Appendix C for details), indicating the absence of sustained flaming within the unit. These results confirm that cavity fires were successfully avoided in the modified UPS system, fulfilling one of the objectives of the enclosure redesign effort noted above.

Although both tests showed similar HRR profiles during the initial 30 minutes, the relocation of flames, from cavity fires in Phase I to external flames in Phase II, significantly increased the distance between the flame and battery modules. This spatial separation reduced heat transfer to the upper modules. In addition, when the sprinklers were activated, the perforated front door was effectively cooled. As shown in Figure 3-11(B), the door temperature dropped from approximately 392 °F (200 °C) to 212 °F (100 °C) at the time of sprinkler activation at ~12 minutes, further reducing heat transfer and preventing TR propagation.

3.3.4 Discussion

As described in Section 3.2.2, only seven modules (Modules 17 and 19 -24) were populated with cells in the Phase II test, while the remaining nine modules (Modules 2, 15, 16, 18, and 25 – 29) were left empty. As shown in Figure 3-11, the modules located directly above the initiating Module 23, such as Modules 19 and 21, are more vulnerable to TR propagation due to the heating from buoyancy-driven flames and high temperature combustion products. However, in the Phase II test, none of the modules above Module 23 experienced TR, indicating that the modified enclosure design effectively prevented upward propagation. This suggests that even if Modules 15, 16, 18, 25, 26, 27, and 28 were fully populated with cells, TR would likely not propagate to them, and the overall HRR history would remain unchanged. Therefore, conducting additional tests with fully populated modules is unlikely to yield new insights into TR propagation trends.

In the Phase II test, simulated thermal links were installed to track the temperature history. Results showed about 5 s difference in the activation time between the 212 °F (100 °C) and 165 °F (74 °C) rated sprinklers, indicating that this difference in activation temperature will not substantially affect the fire-test results.

In addition, heat exposure to potential units across the aisle was evaluated by measuring heat flux at 3 ft away from the unit door in the Phase II test, as shown in Figure 3-12. Flame was located close to the surface of the unit door, and the maximum measured heat flux was 8.1 kW/m^2, which is a low value that does not pose a risk of fire/TR propagation to the units or other materials positioned across the 3 ft aisle.

Based on these findings, the modified UPS system is considered to have passed the FM large-scale fire test.

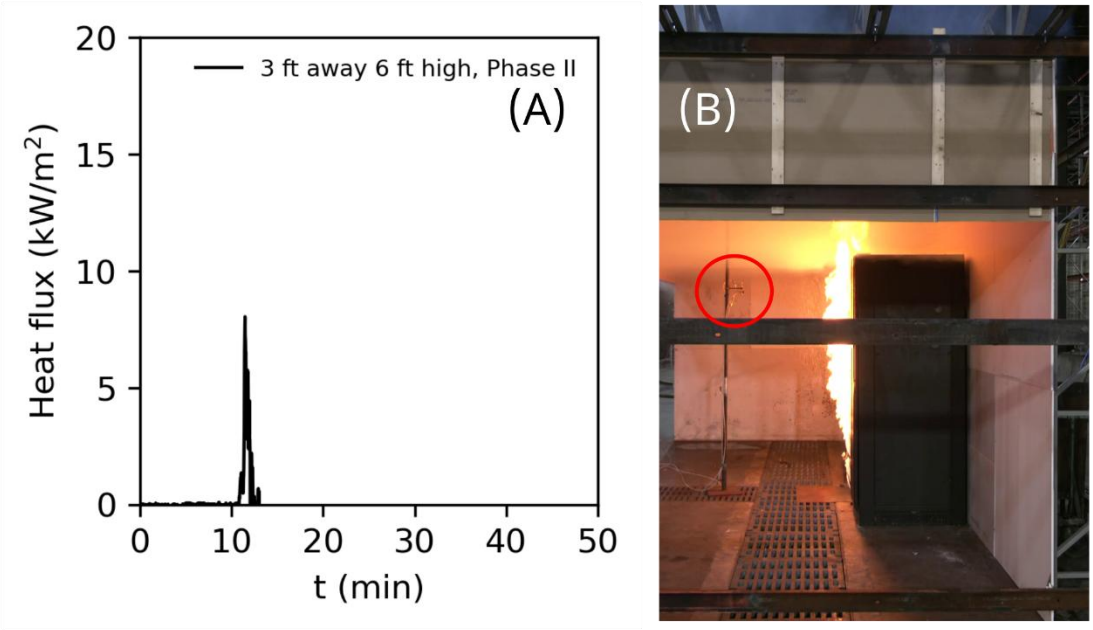

Figure 3-12: Heat flux measurement results in the Phase II test, (A) heat flux history, and (B) image taken at the time of sprinkler activation, with the red circle indicating the location of the heat flux gauge.

4. Evaluation of Explosion Hazard

As the large-scale fire test results demonstrate that TR can be confined to a single module for this specific UPS system design, even under a fire scenario, the explosion hazard analysis is based on the quantity of fuel released by the total number of cells, n_{cells}, contained within a single module. Based on the UL 9540A cell level test [2] for the Delta P140 cell, each cell releases approximately $V_{\text{cell}} = 3.85$ ft^3 (0.1091 m^3) of thermal runaway gas, with a lower flammability limit (LFL) concentration of $C_{\text{LFL}} = 7.35\%$ at ambient temperature.

4.1 Unventilated Scenarios

4.1.1 Unmixed Releases

In an unventilated case without forced mixing, for an explosion event yielding a static overpressure of 1.5 psi (0.1 bar), an explosion model developed by Research at FM, based on thermochemical equilibrium calculations, following an approach similar to that described in [5], yields a critical gas concentration (C_{crit}) of 0.34%. Assuming the flammable cloud formed during the release follows a Gaussian concentration distribution, the optimal cloud center concentration that maximizes (for conservative purposes) the amount of flammable gas that would participate in the explosion is $C_{\text{opt}} = 41\%$, resulting in a maximum participating gas fraction within the cloud of $(Q_{\text{P}}/Q_{\text{T}})_{\text{max}} = 0.59$. The value of $C_{\text{crit}}/(Q_{\text{P}}/Q_{\text{T}})_{\text{max}}$ provides an estimate for the minimum global average room concentration that would present an explosion hazard requiring Damage Limiting Construction (DLC). For this specific case, the value is approximately equal to $C_{\text{LFL}}/13$.

The minimum unoccupied room volume, V_{min}, can then be calculated by the following expression:

$$V_{\text{min}} = \frac{n_{\text{cells}} V_{\text{cell}}}{C_{\text{crit}}} \left(\frac{Q_{\text{P}}}{Q_{\text{T}}}\right)_{\text{max}} = \frac{20 \times 3.85 \text{ ft}^3}{0.0034} \times 0.59 = 13{,}200 \text{ ft}^3 \ (375 \text{ m}^3).$$

This value corresponds to the free volume of the room, which does not include any space occupied by equipment. If major equipment within the room takes up a significant volume, the room size must be increased accordingly.

As a result, the FM explosion hazard model suggests that the full release of all thermal runaway gas from a single module in an unventilated room with a volume at least 13,200 ft^3 (375 m^3), would result in a manageable explosion hazard, limited to localized non-structural damage to the room of origin, without the need for DLC, or any additional ventilation, provided the room is not supported by weak load-bearing wall elements (e.g. unreinforced concrete masonry unit blocks).

4.1.2 Well-Mixed Releases

If internal room circulation or airflow can ensure the release is well mixed, yielding a homogeneous flammable gas concentration throughout the room below a quarter of the LFL, then, in accordance with NFPA 69 [6], the minimum unoccupied room volume could be further reduced to:

$$V_{\text{min}} = \frac{n_{\text{cells}} V_{\text{cell}}}{(C_{\text{LFL}}/4)} = \frac{4 \times 20 \times 3.85 \text{ ft}^3}{0.0735} = 4{,}200 \text{ ft}^3 \ (120 \text{ m}^3).$$

To achieve the well-mixed condition, a minimum airflow across the exterior surface of the racks is needed. For a room volume of 4,200 ft^3 (120 m^3), assuming all thermal runaway gas is released from a single module within 10 minutes, the FM explosion model would require a minimum air flow rate of 0.3 ft/s (0.1 m/s) sweeping across the exterior of the rack. This value decreases linearly with increasing room volume, reaching 0 at the minimum room volume for an unmixed release. It should be noted that this flow does not need to be exhausted from the room and could be achieved using recirculation fans. Furthermore, as a release could occur from any module, this airflow must be provided to all the battery racks present in the room.

4.2 Room Exhaust Ventilation Scenarios

Assuming the same release scenario, one module fully discharging over 10 minutes, the FM explosion model [5] was also applied to scenarios where continuous room exhaust ventilation is provided. For rooms with a height between 11.5 ft (3.5 m) and 16 ft (5 m), and an average room exhaust rate of 1 cfm/ft^2 (0.3 m^3/min/m^2), the model calculates that the minimum unoccupied room volume needed to limit the room explosion hazard:

$$V_{\text{min}} = 8{,}200 \text{ ft}^3 (230 \text{ m}^3).$$

If the average room exhaust rate is increased to 2 cfm/ft^2 (0.6 m^3/min/m^2), for the same range of room heights, the minimum unoccupied room volume can be further reduced to:

$$V_{\min} = 1{,}800 \text{ ft}^3 \ (50 \text{ m}^3).$$

These values assume that continuous room exhaust ventilation is provided uniformly throughout the room, with no stagnant areas near battery racks and there are no localized regions where thermal runaway gas could accumulate. It should be noted that providing both exhaust ventilation and internal room air circulation could further reduce the minimum volume compared to implementing either measure alone. However, the current explosion model formulation does not readily accommodate the combined effect of these assumptions. Future work will focus on updating the FM explosion model to address this limitation.

5. Conclusions

In this work, FM conducted large-scale fire tests involving three LIB UPS units from Delta Electronics Inc. to evaluate fire hazards associated with Li-ion battery UPS systems and to improve the fire safety performance of the UPS system through design modifications. The major test outcomes are:

1. Development of a Realistic Fire Test Protocol:

   A targeted initiation method and large-scale fire test protocol were developed to simulate a realistic failure scenario under representative conditions. The current testing protocol, which features the intentional ignition of TR vent gases, represents a reasonably conservative scenario and is more effective at evaluating fire hazards than existing protocols. Notably, while the original UPS system did not exhibit fire spread hazards under UL 9540A test conditions, it failed the FM large-scale fire test. These results suggest that FM's test method could serve as the foundation for a standardized fire testing procedure for UPS battery systems.

2. Fire Propagation Observed in Phase I Test:

   In the Phase I test with three original UPS units, combustible gases released from the initiating module burned within the unit enclosure, forming cavity fires. These fires provided sufficient heat to induce TR in adjacent modules, leading to fire propagation within the initiating unit. Temperature data from the neighboring target units indicated elevated module surface temperatures, suggesting imminent TR propagation. Although the sprinklers were activated during the test, the enclosure design of the unit significantly limited water access, reducing the effectiveness of cooling and fire suppression.

3. Implementation of Mitigation Strategies:

   Based on the Phase I test results, several design modifications were implemented to mitigate TR propagation risks. These include: 1) Compartmentalizing each battery module and perforating the unit door to redirect vent gases and reduce cavity fire formation, 2) Removing the interior side panel walls of the adjacent units to improve heat dissipation and enhance sprinkler cooling effectiveness, and 3) Adding insulation between adjacent modules to reduce inter-module heat transfer and limit TR propagation.

4. Successful Mitigation of TR Propagation in Phase II Test:

   In the Phase II test with the modified UPS unit, the same initiation method as in the Phase I test was used, and a similar initial HRR profile was recorded. However, TR did not propagate beyond the initiating module. The test results confirmed that cavity fires were avoided, fulfilling the objective of the design modification. The modified UPS system successfully passed the FM large-scale fire test.

5. Explosion Hazard Analysis:

   The explosion hazard was evaluated under the scenario in which one full module undergoes TR. FM's proprietary models calculate that this release would not present a significant room explosion hazard, limited to localized non-structural damage in the room of origin, and Damage Limiting Construction (DLC) would not be required, when installed in a room with an unoccupied volume greater than approximately 13,200 ft^3 (375 m^3) even without any supplemental ventilation or airflow. If 2 cfm/ft^2 (0.61 $m^3/min/m^2$) of continuous room exhaust ventilation were provided and arranged for reliable operation, this volume could be further reduced to approximately 1,800 ft^3 (50 m^3).

In conclusion, the FM large-scale fire test method effectively captures realistic failure scenarios involving external ignition and module-level thermal runaway failure, offering a more conservative and representative evaluation of fire hazards in Li-ion battery UPS systems. The methodology provides a strong foundation for future standard development.

Design enhancements developed through technical engagement among FM, Delta, and Equinix resulted in significant design improvements to the fire safety performance of the Delta LIB UPS systems. The modified system described in Section 3.3.2 successfully passed the FM fire test, demonstrating its ability to contain thermal runaway and prevent fire propagation, making a substantial advancement in UPS fire safety.

Nomenclature and Abbreviations

Nomenclature

c	specific heat capacity (J g^{-1} K^{-1})
C_{LFL}	lower flammability limit concentration
C_{crit}	critical gas concentration
C_{opt}	optimal cloud center gas concentration
m	mass (g)
$\dot{m}_o$	mass consumption rate of oxygen measured in the calorimeter (g/s)
n_{cells}	number of cells underwent thermal runaway
$\dot{Q}$	heat gain/loss rate (W)
$\dot{Q}_c$	combustion heat release rate (kW)
Q_{IHG}	internal heat generation (J)
$(Q_{\mathrm{P}}/Q_{\mathrm{T}})_{\mathrm{max}}$	maximum participating gas fraction within the cloud
T	temperature (K)
V_{cell}	volume of released gas from thermal runaway of one battery cell (m^3)
V_{min}	minimum unoccupied room volume (m^3)
$\overline{\Delta H_o}$	weighted average of the net heat of combustion per unit mass of oxygen consumed (kJ/g)

Abbreviations

AHJs	Authorities Having Jurisdiction
DLC	Damage Limiting Construction
HRR	heat release rate
LFL	lower flammability limit
LIBs	lithium-ion batteries
NMC	lithium nickel manganese cobalt oxide
SOC	state-of-charge
TR	thermal runaway
UPS	uninterruptible power supply

References

[1] ANSI/CAN/UL 9540A, Standard for Safety: Test Method for Evaluating Thermal Runaway Fire Propagation in Battery Energy Storage Systems, UL Inc., 2025.

[2] TUVRheinland, UL 9540A Unit Level Test (2019, fourth edition) Report for Delta Electronics Cell Level Test Report, 2020.

[3] TUVRheinland, UL 9540A Unit Level Test (2019, fourth edition) Report for Delta Electronics BSPRU-DE1xx2P0GL0 Indoor Battery Cabinet, 2024.

[4] ANSI/CAN/UL 9540A, Standard for Safety: Test Method for Evaluating Thermal Runaway Fire Propagation in Battery Energy Storage Systems, UL LLC., 2019.

[5] C.R.L. Bauwens, M. Chaos, S.B. Dorofeev, Estimating the Minimum Quantity of Fuel Needed to Pose a Room Explosion Hazard. In. Proceedings of the 16th International Symposium on Hazards, Prevention, and Mitigation of Industrial Explosions; April 20-24, 2026; Kaohsiung, Taiwan.

[6] NFPA 69, Standard on explosion prevention systems, National Fire Protection Association, 2024.

[7] G. Xiong, C. Chak, W. Brown, D. Zeng, R. Barlow, Y. Wang, A calorimeter for quantifying thermal runaway dynamics in pouch cells, Fire Saf. J. 162 (2026) 104698. doi: 10.1016/j.firesaf.2026.104698.

[8] P. Garg, G. Xiong, L. Gagnon, D. Zeng, Y. Wang, R. Barlow, Measurement of Total and Temporal Heat Generation Carried by Ejected and Non-Ejected Contents during Thermal Runaway of 18650 Lithium-ion Batteries. In: P. Russo, M.C. Lancia. Proceedings of the 11th International Seminar on Fire and Explosion Hazards; June 15-20 2025; Rome, Italy.

[9] M.M. Khan, A. Tewarson, M. Chaos, Combustion characteristics of materials and generation of fire products, in: M.J. Hurley, D.T. Gottuk, J.R. Hall Jr, K. Harada, E.D. Kuligowski, M. Puchovsky, J.M. Watts Jr, C.J. Wieczorek (Eds.), SFPE Handbook of Fire Protection Engineering, Springer, 2016, pp. 1143-1232. doi: https://doi.org/10.1007/978-1-4939-2565-0_36.

[10] L. Gagnon, D. Zeng, B. Ditch, Y. Wang, Cell-level thermal runaway behavior of large-format Li-ion pouch cells, Fire Safety J. 140 (2023) 103904. doi: https://doi.org/10.1016/j.firesaf.2023.103904.

Appendix A. Initiation Design for Large-scale Fire Test

Half of the cells in a module, i.e., 10 cells, were induced to TR as the initiation scenario. Due to space limitations within the module, flexible sheet-type heaters (McMaster-Carr part no. 35765K644) were employed to activate multiple cells in one module into TR. The heaters measure 24 inches in length, 2 inches in width, and 0.07 inches in thickness (609 × 51 × 1.8 mm), providing 480 W each at 120 volts AC, with a maximum operating temperature of 490°F. Figure A-1(A) illustrates the placement of two heaters on the inner large faces of Cells 2, 6, 10, 14, and 18, as well as two heaters on the inner large faces of Cells 3, 7, 11, 15, and 19, arranged as depicted in the figure. Figure A-1(B) illustrates that two independent power sources (Variacs) supplied a constant voltage to heaters arranged in parallel.

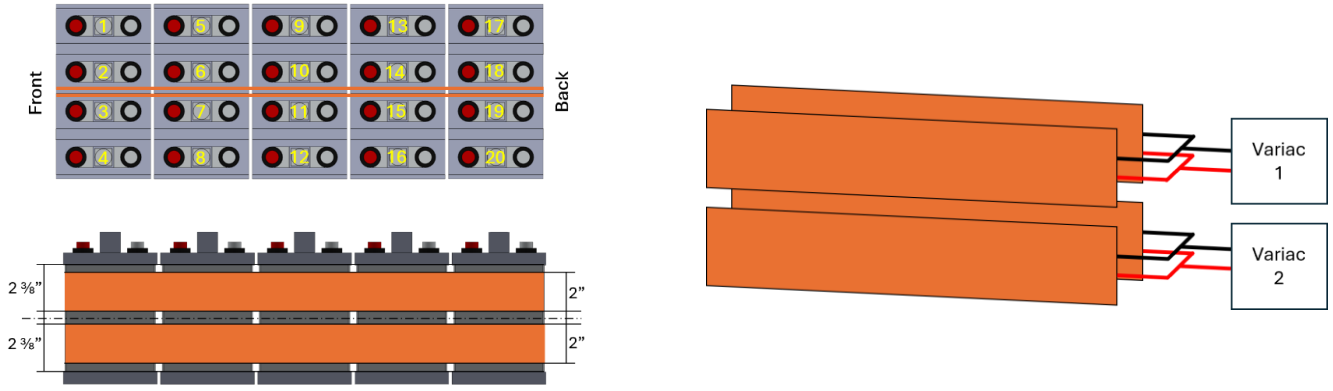

(A) Heater placement (B) Heater power supply

Figure A-1: Heater setup in the initiating module.

The TR initiation design was evaluated with a two-module test, as shown in Figure A-2. A glow plug was positioned between the front face of the module and the mock-up door to ignite the flammable gases produced during TR, aligning with the gap between the module's top cover and the rack tray. A supplementary glow plug and premixed pilot flame were also implemented at 1 ft above the first glow plug. The test assembly was placed under a calorimeter to measure HRR.

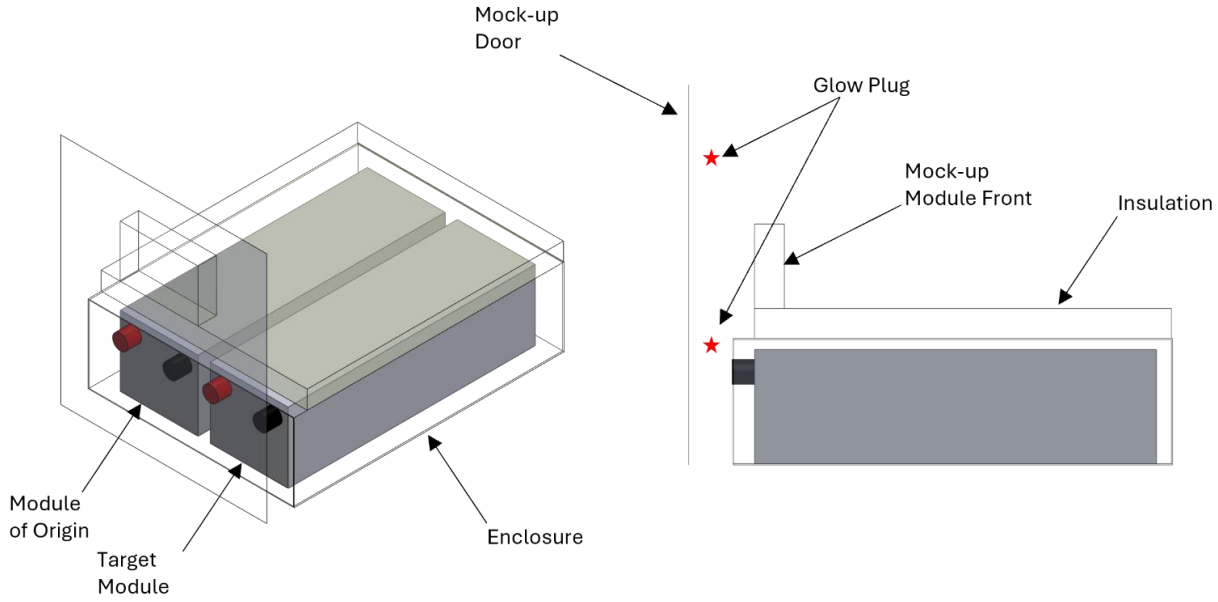

Figure A-2: Sketch of the module-level test setup to evaluate the TR initiation method.

Appendix B. Cell-level Characteristics

The cell-level test focused on quantifying fire hazard characteristics, including combustion heat release, internal heat release, and TR onset temperature. In the cell-level test, the LIB cell was positioned between a copper plate heater and a copper plate heat sink, with both plates insulated by a 1-inch-thick (25.4 mm) layer of insulation (Marinite board) on each side, as shown in Figure B-1.

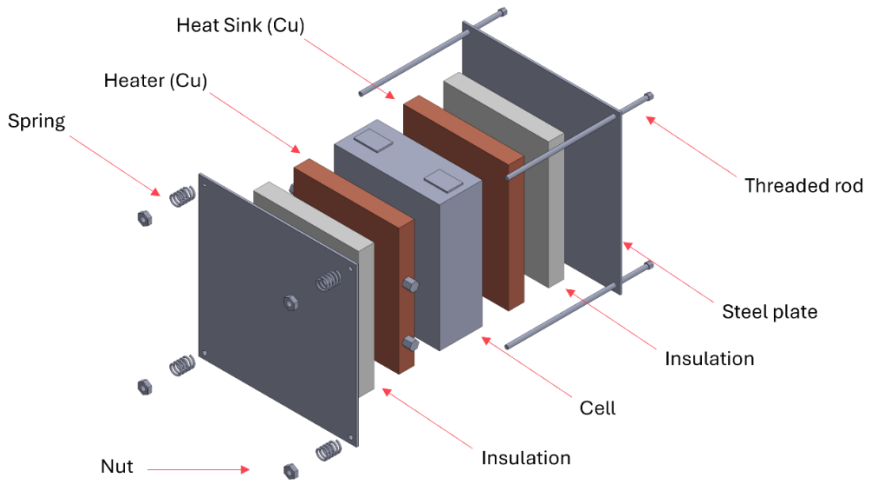

Figure B-1: Cell-level test setup.

The copper elements and the insulation were cut to match the cross-section of the cells, ensuring uniform thermal contact and insulation. The copper plate heater had a thickness of 0.5 inches (12.7 mm). Four cartridge heaters (Tempco swaged cartridge heaters, 400 W each, maximum temperature of 1200 °F, McMaster-Carr part no. 6455N28) were embedded into the copper heater. Two independent power sources (Variacs) were used to provide a constant voltage to the cartridge heaters. Each source controlled two heaters, which were wired in parallel. The copper plate heat sink had a thickness of 0.25 inches (6.4 mm) and was positioned on the opposing face of the cell to capture some of the heat generated during TR. Two steel plates, each 0.25 inch thick, were employed to secure the insulation, heater, cell, heat sink, and insulation layer stack, with a consistent torque applied to each of the four bolts fastening the assembly. Table B-1 presents the initial mass and dimensions of the cells, along with the components of the cell test setup.

Table B-1: Mass and Dimensions of Cells, Copper Plates, Insulation, and Steel Plates

	Initial Mass [lb] ([kg])	Height [in] ([mm])	Width [in] ([mm])	Thickness [in] ([mm])
LIB cell	3.1 (1.4)	6.1 (155.6)	4.3 (110.1)	1.50 (38.2)
Heater Cu plate	3.9 (1.8)		4.3 (110.1)	0.50 (12.7)
Cold Cu Plate	1.9 (0.9)		4.3 (110.1)	0.25 (6.4)
Marinite board	0.9 (0.3)		4.3 (110.1)	1.00 (25.4)
Steel Plate	1.7 (0.8)		6.3 (160.1)	0.25 (6.4)

A glow plug was positioned 1 inch (25.4 mm) above the cell to ignite the vented gases, while a second glow plug was installed 1 foot (305 mm) above the cell as a fail-safe ignitor, accompanied by a premixed propane/air pilot flame. The entire test configuration was positioned beneath the 1 MW calorimeter at the FM Research Campus Small Burn Lab to measure the chemical HRR.

The instrumentation is shown in Figure B-2. Three type-K thermocouples (0.062 inches, 1.56 mm, OD) were integrated into each of the heater and heat sink copper plates to monitor their temperature. Additional thermocouples were installed on the cell surfaces facing the heater and heat sink plates, on each insulation layer, and on the faces of each steel plate.

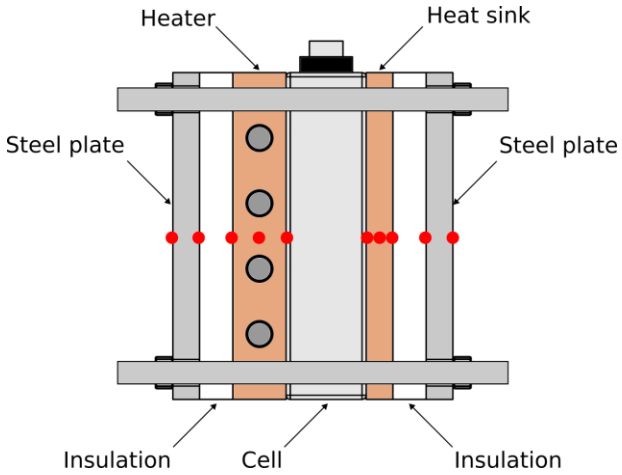

Figure B-2: Illustration of placement of thermocouples (red dots) in the cell-level test setup.

Figure B-3 shows the temperature histories recorded by the thermocouples throughout the TR test. The venting and TR onset temperatures are 500 °F (260 °C) and 507 °F (264 °C), respectively. Prior to 969 seconds, the temperature of the heater increases due to electric heating, and the temperature on cell side 1 (in contact with the heater) closely aligns with the heater's temperature. Heat transfer within the cell results in an increase in temperature at cell side 2 (in contact with the heat sink), and the temperatures of the other components also increase correspondingly. At 969 seconds, TR occurs, resulting in a rapid temperature increase in the cell, heater, and heat sink due to the heat generated from exothermic reactions. The heater's electrical power is deactivated after approximately 1000 seconds. Subsequently, the temperatures of the heater, cell, and heat sink progressively converge towards thermal equilibrium.

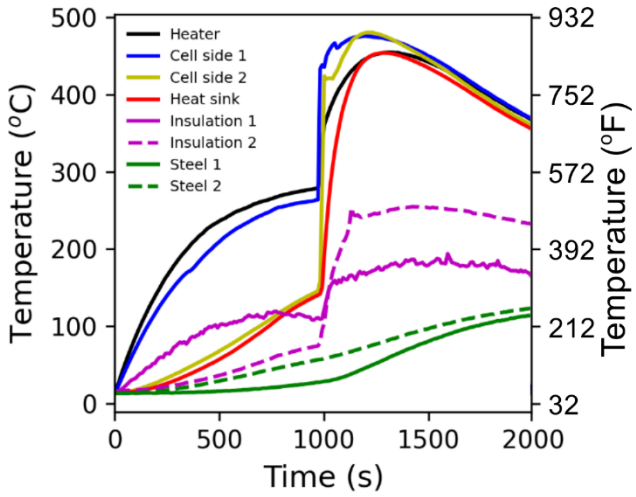

Figure B-3: Temperature history of thermocouples at locations indicated in the legend; side 1 represents the heater side, and side 2 represents the heat sink side.

Internal heat generation (Q_{IHG}), which stems from the exothermic thermal runaway reactions occurring within the battery cells, represents an additional thermal hazard, which was characterized in this study. Q_{IHG} was determined using the temperature data recorded during the thermal runaway process in the single-cell test, following the methodology established in a prior single-cell study [7]. An energy balance analysis was performed to determine Q_{IHG}, utilizing a control volume that encompassed the steel plates, both insulation layers, the copper plate heat sink, the heater copper plate, and the cell. The transient energy equation for this control volume is

$$\sum_{\mathrm{k}} m_{\mathrm{k}} c_{\mathrm{k}} \frac{\mathrm{d}T_{\mathrm{k}}}{\mathrm{d}t} + m_{\mathrm{b}} c_{\mathrm{b}} \frac{\mathrm{d}T_{\mathrm{b}}}{\mathrm{d}t} = \dot{Q}_{\mathrm{ht}} + \dot{Q}_{\mathrm{IHG}} - \dot{Q}_{\mathrm{ls}} ,$$

where, m is the mass (g), c is the specific heat capacity (J g^{-1} K^{-1}), T is the temperature (K), $\dot{Q}$ is the heat gain/loss rate (W), the subscripts b, ht, IHG, and ls denote battery, heater input, internal heat generation, and heat loss, respectively. The subscript k denotes the various inert components within the control volume, which include heater-side (hot) insulation, heater (hot) copper plate, heat sink (cold) copper plate, heat-sink-side (cold) insulation, and hot and cold sides of steel plates. The energy equation signifies that the total power input, comprising heater input and internal heat generation, minus heat loss, equals the change in sensible enthalpy of the materials. TR is a complex process involving internal chemical reactions and the ejection of multi-component materials from the control volume. Consequently, certain assumptions are made to derive this general energy equation, for instance, it is assumed that the ejected materials possess identical specific heat capacity and temperature as the cell [8].

Figure B-4 plots the calculated internal heat release rate ($\dot{Q}_{\mathrm{IHG}}$) throughout the TR process. The maximum $\dot{Q}_{\mathrm{IHG}}$ attained a value of approximately 29 kW. The value of Q_{IHG}, determined by integrating $\dot{Q}_{\mathrm{IHG}}$, was 0.65 MJ, which is approximately 19% lower than the nominal electrical energy of the cell, 0.8 MJ.

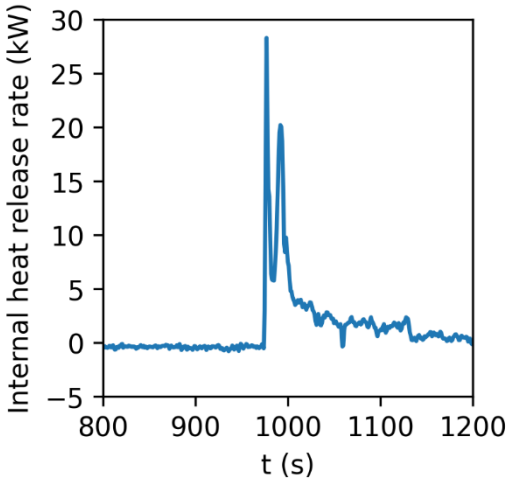

Figure B-4: Internal heat generation rate from a cell.

In addition to the internal heat release, the combustion HRR was obtained from the 1 MW calorimeter measurement based on oxygen consumption calorimetry [9]:

$$\dot{Q}_c = \dot{m}_o \overline{\Delta H_o},$$

where $\dot{m}_o$ (g/s) is the mass consumption rate of oxygen measured in the calorimeter during a test, and $\overline{\Delta H_o}$ (kJ/g) is the weighted average of the net heat of combustion per unit mass of oxygen consumed for the combustible gas species present in the product emissions from a cell during TR [10]. A value of 12.8 kJ/g is commonly used for $\overline{\Delta H_o}$, but this value is based on an average of various common hydrocarbon fuels [9]. Presently, the UL 9540A cell test report [2] documents the composition of the TR effluent gas, as shown in Table B-2. Except for carbon dioxide, all other gas species are combustible. Using this data, we derived a value of 14.7 kJ/g for $\overline{\Delta H_o}$.

Figure B-5 presents the HRR obtained from the 1 MW calorimeter measurement. During this test, venting commenced approximately 75 seconds before TR, which occurred at around 969 seconds; however, the vented gas did not ignite. The ignition occurred upon the start of TR, followed by a rapid ejection of effluent gas that resulted in a local maximum HRR, as illustrated in Figure B-6(A). The fire size decreased briefly before transitioning into another large fire that lasted approximately 60 seconds, subsequently reducing to small, lingering flames. Figure B-6(B) presents a fire image associated with the second local HRR maximum depicted in Figure B-5. The peak HRR attained was approximately 170 kW. The total chemical heat release, determined by integrating the HRR data, was 3.7 MJ.

Table B-2: Components measured in vented TR effluent gas [2].

Gas	Formula	Volume fraction (%)
Carbon Monoxide	CO	26.25
Carbon Dioxide	CO_2	24.59
Hydrogen	H_2	35.7
Methane	CH_4	4.36
Ethylene	C_2H_4	3.91
Ethane	C_2H_6	0.83
Propylene	C_3H_6	2.57
Propane	C_3H_8	0.33
Propadiene	C_3H_4	0.02
Total C_4 (assume n-butane)	C_4H_{10}	1.28
Pentane	n-C_5H_{12}	0.11
Isopentane	C_5H_{12}	0.03
Hexane	C_6H_{14}	0.02
Total	-	100

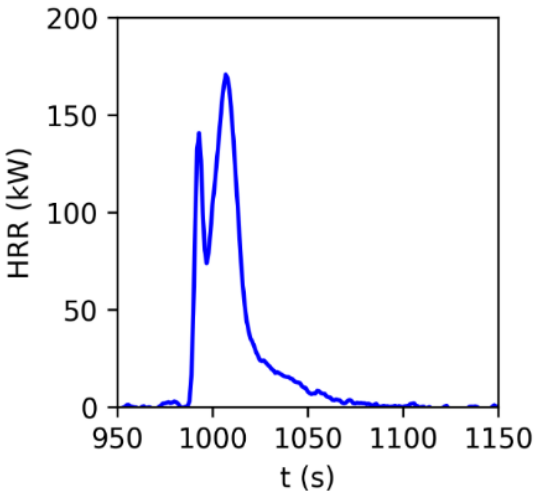

Figure B-5: Heat release rate of the cell-level fire test.

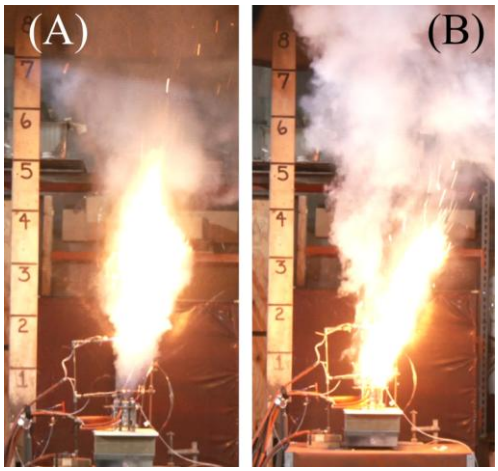

Figure B-6: Flame image approximately corresponding to the first (~971 s) and second (~978 s) local maxima HRR in Figure B-5.

In summary, cell-level characterization shows that the chemical heat release is 3.7 MJ, internal heat release is 0.65 MJ, the venting temperature is 260 ℃, and the thermal runaway onset temperature is 264 ℃. These are significant parameters for assessing the fire hazard associated with a specific cell. These values are particularly useful for comparing the cell hazards in future potential cell replacements with a similar module design. Chemical heat release is also a critical parameter for assessing explosion hazards in cases of a delayed ignition.

Appendix C. Detailed Instrumentation for Large-scale Fire Test

Figure C-1 shows the instrumentation utilized in the Phase I large-scale fire test. These instruments are designed to assess the status of fire propagation within the unit of origin and the thermal exposure of the fire to surrounding areas, including adjacent units and compartment walls. Figure C-1(A) presents a front-view schematic depicting the installation of thermocouples on the unit of origin for Phase I.

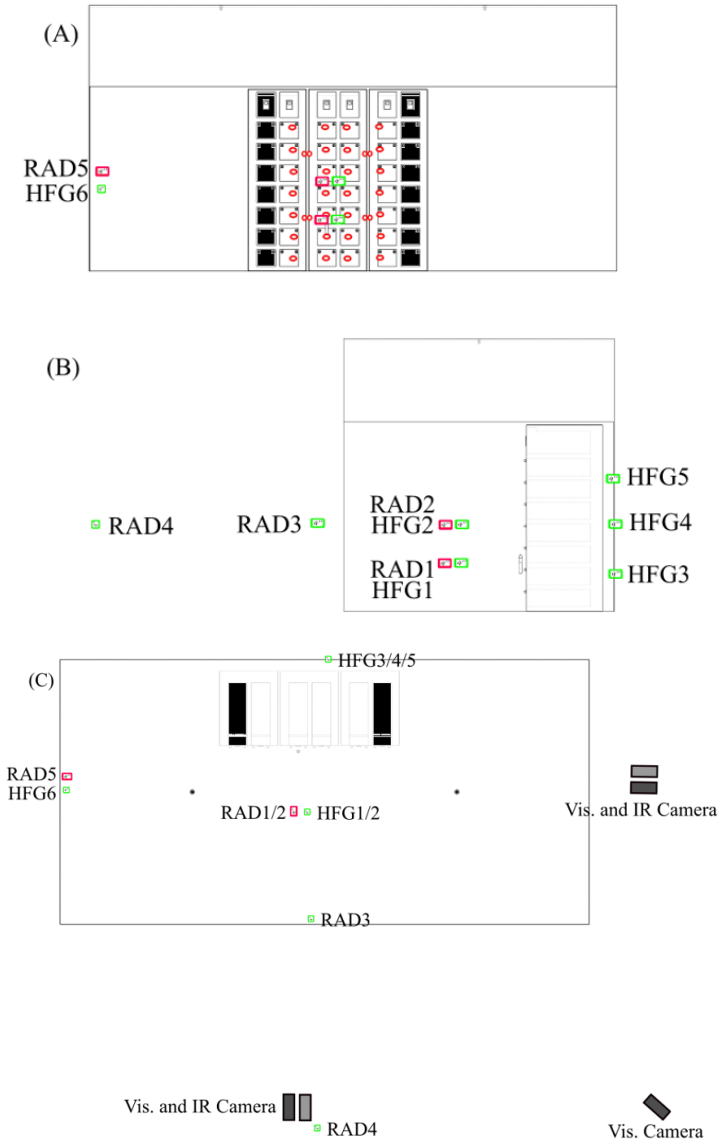

Figure C-1: Schematic of the large-scale test instrumentation layout in Phase I test: (A) front view schematic, the red circles represent thermocouples, (B) side view schematic, (C) plan view of the rack of origin and adjacent racks.

Thermocouples were installed on the front and back surfaces of the modules, as shown in Figure C-2. In the unit of origin, thermocouples were placed in the center of the front and back surface. In the target units, the thermocouples were positioned aligned with the row of cells closest to the unit of origin.

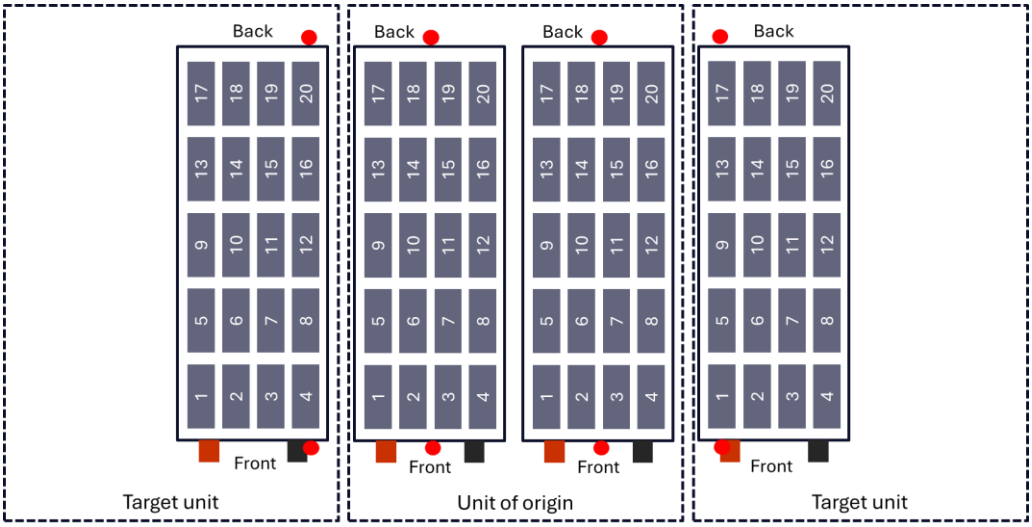

Figure C-2: Illustration of thermocouple placements for the modules in the Phase I test.

In the Phase II test, four thermocouples were placed on the walls of the target units to evaluate their response. The thermocouples were at the heights of Module 21 and Module 15, as shown in Figure C-3. The upper thermocouple of the right unit was damaged during the fire test, which impacted data collection.

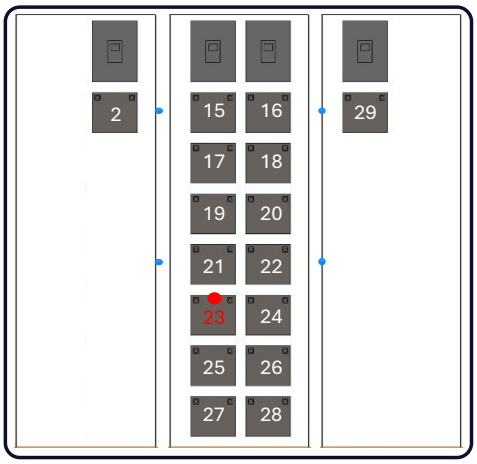

Figure C-3: Thermocouple locations on the wall of target units in Phase II test, with blue dots showing the locations of the thermocouples.

The modified version of the unit has a perforated structure on the front door to allow flammable gases to vent. To evaluate the effect of flame exposure and the cooling effectiveness of sprinkler water, eight thermocouples (TCs) were installed on the inner side of the front door, as shown in Figure C-4. Dashed rectangles mark the locations of the modules. The eight TCs were positioned directly above the center of Modules 17 – 24.

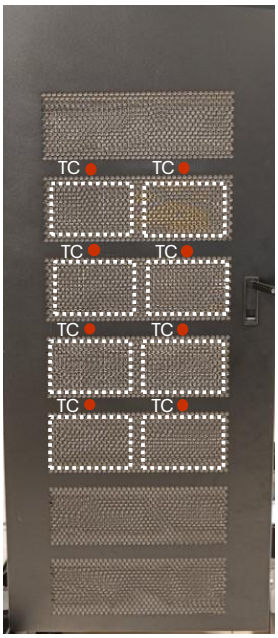

Figure C-4: Illustration of placement of thermocouples (TCs) on the front perforated door of the unit of origin in Phase II test, with dashed rectangles marking the location of the modules.

Appendix D. Experimental Observations

Figure D-1 presents representative images illustrating the major stages of the Phase I fire test. Figure D-1(A) shows the three battery units prior to the test initiation. Approximately 17 minutes after the test commenced, following the activation of the tape heaters in Module 23, flames were observed emerging from the top surface and door seams of the initiating unit (refer to Figure D-1(B)). This observation signifies the onset of TR in Module 23 and the ignition of vent gases by the glow plugs. The West sprinkler (see Figure 3-3) was activated by the flame approximately 20 seconds after it became visible outside the units, with the East sprinkler activating about two minutes later. The interaction between the fire and sprinkler water produced significant smoke and vapor, as shown in Figure D-1(C). The external flaming condition persisted for around five minutes (17-22 minutes); after which the smoke dissipated. At around 29 minutes (refer to Figure D-1(D)), flames reappeared, indicating the propagation of fire and TR from Module 23 to adjacent modules. Subsequently, the fire size continued increasing, with flames emerging from the partially open side walls at approximately 40 minutes; refer to Figure D-1(E). Following this stage, fire heating compromised the ceiling structure, resulting in partial collapse, with flames emerging from the upper section of the compartment, as illustrated in Figure D-1(F).

Figure D-2 presents representative images illustrating the progression of the Phase II fire test. Figure D-2(B) shows the image approximately three seconds after ignition at around 11 minutes after the start of the test. At this stage, the flame stayed in front of the unit door. Sprinklers were activated at approximately 12 minutes, with Figure D-2(C) and (D) showing the images immediately before and after the sprinkler activation. The flame persisted but remained weak until about 13.5 minutes, at which point it was no longer visible. However, the flame reignited outside the unit door around 14.5 minutes. From approximately 15.5 minutes onward, the flame remained small and was no longer observed after 24 minutes. The test configuration was monitored for 24 hours for any thermal runaway, as one of the two criteria, to confirm that the fire hazard was confined to the unit of origin. No thermal runaway was observed as expected from the test data.

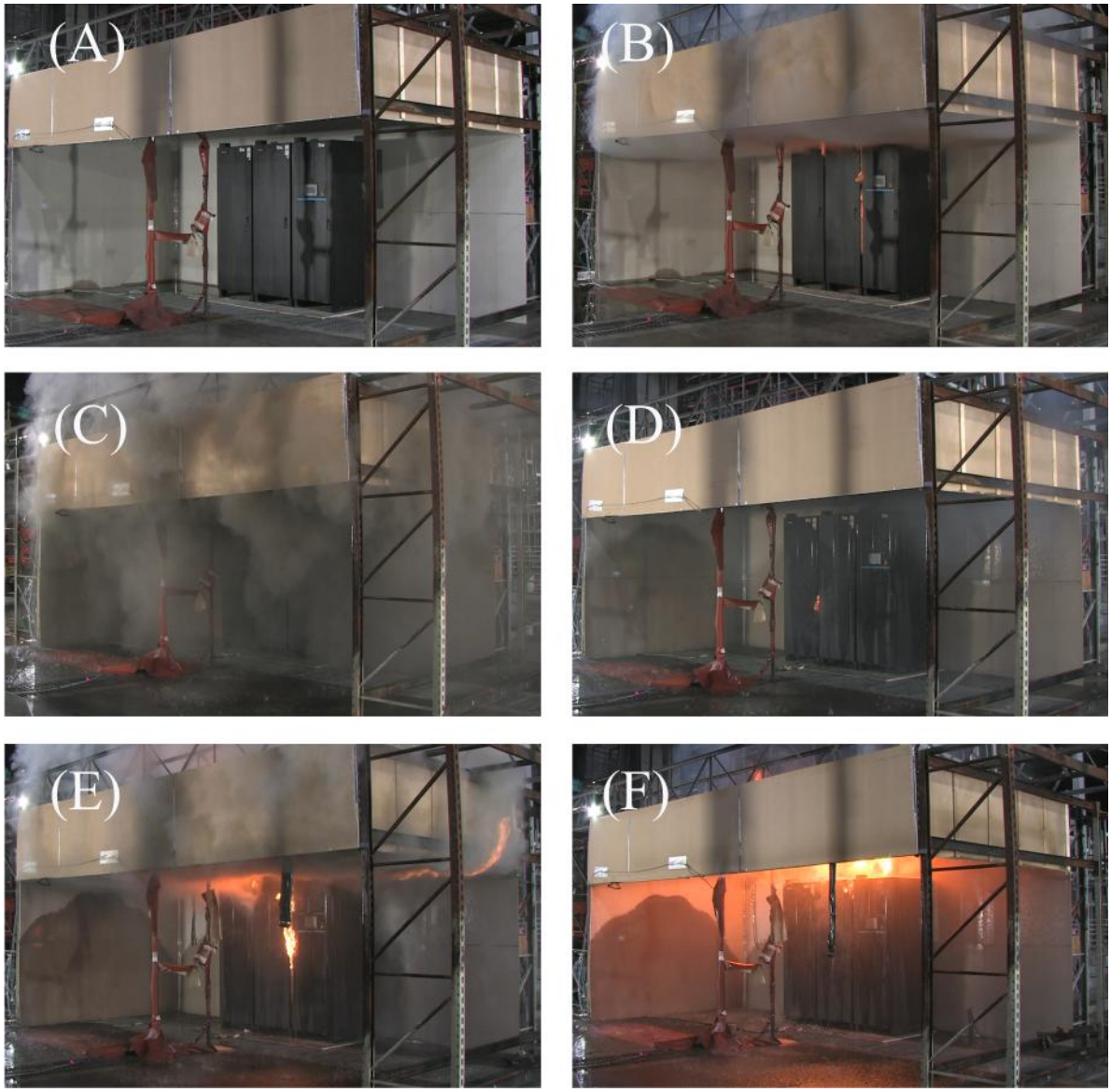

Figure D-1: Representative images of the Phase I fire test: (A) pretest, (B) at approximately17 minutes flames emerge from the top surface and door seams of the initiating unit, (C) sprinkler activation at around 24 minutes, (D) ~29 minutes, reignition is observed with flames emerging from the initiating unit, (E) ~40 minutes, fire size increases and flames emerge from the partially open side walls, (F) ~42 minutes, fire heating damaged the ceiling structure, causing partial ceiling collapse, and flames emerge from the top of the room.

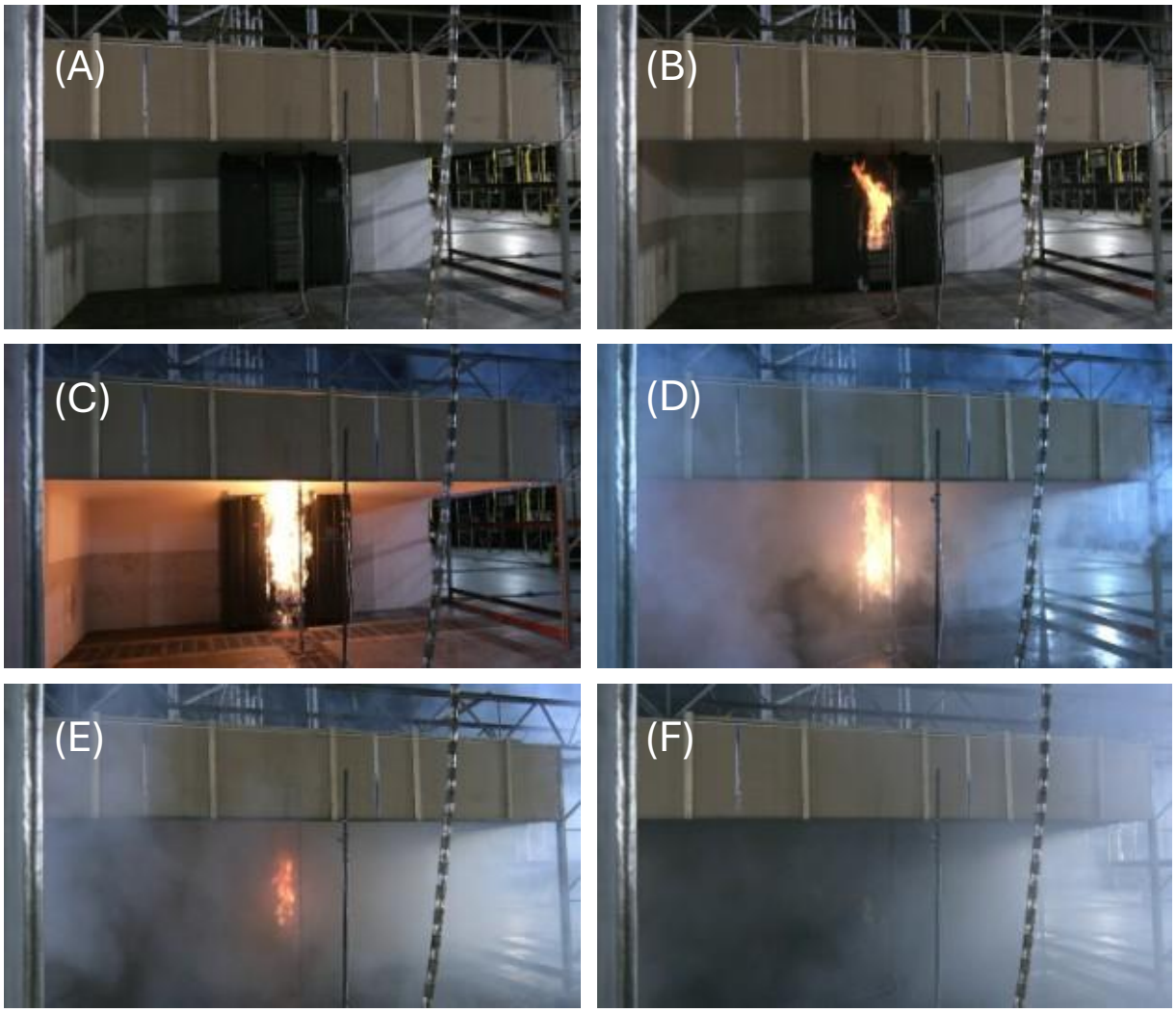

Figure D-2: Representative images of the Phase II fire test: (A) pretest, (B) 3 s after ignition, flames stayed in front of the unit door, (C) 3 s before sprinkler activation, (D) 3 s after sprinkler activation, (E) 13 minutes, flame persisted in front of the unit door and became weak, (F) 24 minutes, no more flames observed.

FM

InsurerFM

FMGlobal

TheFMGroup